J Mater Sci (2008) 43:494–502
DOI 10.1007/s10853-007-1875-4

5TH BRAZILIAN MRS MEETING

Sol–gel derived composite from bioactive glass–polyvinyl alcohol

Hermes S. Costa · Magda F. Rocha · Giovanna I. Andrade · Edel F. Barbosa-Stancioli · Marivalda M. Pereira · Rodrigo L. Orefice · Wander L. Vasconcelos · Herman S. Mansur

Received: 29 January 2007 / Accepted: 22 May 2007 / Published online: 27 July 2007

Abstract Investigation of novel biomaterials for bone engineering is based on the development of porous scaffolds, which should match the properties of the tissue that is to be replaced. These materials need to be biocompatible, ideally osteoinductive, osteoconductive, and mechanically well-matched. In the present paper, we report the preparation and characterization of hybrid macroporous scaffold of polyvinyl alcohol (PVA)/bioactive glass through the sol–gel route. Hybrids containing PVA (80, 70 and 60 wt%) and bioactive glass with composition $58SiO_2$–$33CaO$–$9P_2O_5$ were synthesized by foaming a mixture of polymer solution and bioactive glass via sol–gel precursor solution. PVA with two different degree of hydrolysis (DH), 98.5% (high degree) and 80% (low degree) were also investigated, in order to evaluate the influence of residual acetate group present in polymer chain on the final structure and properties of 3D porous composite produced. The microstructure, morphology and crystallinity of the hybrid porous scaffolds were characterized by X-ray diffraction (XRD), Infrared Fourier Transform spectrometry (FTIR) and Scanning electron microscopy (SEM/EDX) analysis. In addition, specific surface area was assessed by B.E.T. nitrogen adsorption method and mechanical behavior was evaluated by compression tests. Preliminary cytotoxicity and cell viability were also performed by the MTT assay. VERO cell monolayers were grown in 96-well microtiter plates. The results have clearly showed that hybrid foams of polyvinyl alcohol/bioactive glass (PVA/BG) with interconnected macroporous 3D structure were successfully produced. All the tested hybrids of PVA/BG have showed adequate cell viability properties for potential biological applications.

H. S. Costa · M. F. Rocha · M. M. Pereira · R. L. Orefice · W. L. Vasconcelos · H. S. Mansur (✉)
Department of Metallurgical and Materials Engineering, Laboratory of Biomaterials and Tissue Engineering, Federal University of Minas Gerais, R. Espírito Santo 35, Belo Horizonte CEP 30160-030, Brazil
e-mail: hmansur@demet.ufmg.br

G. I. Andrade · E. F. Barbosa-Stancioli
Department of Microbiology, Institute of Biological Sciences, Federal University of Minas Gerais, PO Box 486, Belo Horizonte, MG 31270-901, Brazil

Introduction

Regenerative biology promises to be one of the biomedical revolutions of the 21st century. It encompasses three research approaches: implantation of bioartificial tissues, cell transplantation, and stimulation of regeneration from residual tissues in vivo. Several materials have been developed with the objective of regeneration or substitution of bone tissue structures injured or lost by diseases or accidents. However, a gap remains to be filled since no synthetic material used until now presents characteristics close to the natural tissue, attending both biological aspects as well as mechanical requirements [1–8]. Among these materials bioactive ceramics have been largely studied and used due to their osteoconduction properties and the ability of promoting the formation of a continuous bone–ceramic interface, therefore allowing an implant fixation mechanism. Bioceramics usually have mechanical properties quite different from those of natural tissues, particularly a high elastic modulus and a low toughness. Bioactive glasses are important bioceramic materials and have been used for the repair and reconstruction of diseased bone tissues. The so-called bioactive glasses

promote bone-tissue formation at their surface and bond to surrounding living tissue when implanted in the living body. A common characteristic of bioactive materials is the formation of an apatite-like layer on their surface when they are in contact with physiological fluids or solutions that mimic human plasma [6–10]. However, bioactive glasses have low mechanical properties, especially in a porous form, compared to cortical and cancellous bone [9, 10]. This fact restricts the use of these materials in a wide range of applications. One alternative that is being considered and studied is the production of composites and hybrid systems. Hence, the development of organic–inorganic (O–I) hybrids is regarded as a promising approach for preparing bioactive scaffolds [10]. Polymer composites, which include a bioactive glass phase, have the potential capability of combining bioactive behavior with adequate mechanical properties. More specifically, composite materials based on biodegradable polymers such PVA associated with inorganic bioactive glasses are of particular interest to engineered scaffolds because they offer an excellent balance between strength and toughness and also improving mechanical properties when compared to their individual components [11–14]. In recent years, particular attention was paid to the synthesis of bioceramics and composites with porous morphology to allow the in-growth of bone tissue [3, 6–8]. The appropriate porosity and bioactivity allows the adhesion, nucleation and growth of bone tissue to achieve full integration with the living bones. The chemical composition of the tissue engineered scaffold is crucial for the resorbability and osteoconductive properties together with its internal porous structure for the vascular growth [9, 13]. The major aspects that affect the osteoconduction in the porous materials are the pore size, pore shape, pore connectivity, and bioactivity [4]. Ideally, from the bone tissue engineering design approach, the biomaterial should support compressive loading and tensile or torsion stresses, presenting similar mechanical property compatible with the natural bone tissue. In addition to that, the 3D scaffold should be biocompatible, osteoinductive, osteoconductive with a highly interconnected porous structure. Finally, it must also induce cell anchorage and remodel the extracellular matrix in order to integrate with the surrounding tissue. Thus, despite of the complexity of the system, such challenges have to be overcome in order to achieve proper replacement of bone tissues by synthetic materials [6, 9].

In summary, the present work aimed to have synthesized and characterized O–I hybrids based on bioactive glass obtained via the sol–gel method modified with different contents of PVA. The effect of major synthesis parameters such as degree of hydrolysis of PVA, initial concentration of PVA solution and different PVA/BG composition ratios on the final properties of composites was also investigated. In addition to that, preliminary cytotoxicity assay was conducted. As far as we are concerned, this is the first report in the literature where 3D porous scaffolds based on hybrids of PVA/BG with different degree of hydrolysis were synthesized and extensively characterized, and also several polymer/glass ratios were systematically investigated.

Materials and methods

Synthesis of BG/PVA hybrids

Hybrids containing PVA (80, 70 and 60 wt%) and bioactive glass with composition $58SiO_2$–$33CaO$–$9P_2O_5$ were synthesized by foaming a mixture of polymer solution and bioactive glass sol–gel precursor solution and used for the cytotoxicity studies. Two different degree of hydrolysis PVA were used: Celvol 103, degree of hydrolysis 98.0–98.8% (PVA-98.5), average molecular weight (M_w) = 13,000–23,000 g/mol and from Aldrich-Sigma, degree of hydrolysis 80% (PVA-80), M_w = 9,000–10,000 g/mol. PVA aqueous solutions were prepared by dissolving the PVA powder in a water bath at 80 °C, under moderate stirring, for 2 h. In other to evaluate the influence of hydrophilic polymer initial concentration on stabilizing the foam formation, PVA aqueous solutions were prepared with two different concentrations, 28% and 35% (weight%). The starting sol solution was synthesized from mixing tetraethoxysilane (TEOS, Sigma), D.I. water, triethylphosphate (TEP, Sigma), and calcium chloride ($CaCl_2 \cdot 2H_2O$, Fluka) in presence of hydrochloric acid solution 2 N. The H_2O/TEOS molar ratio used was 12:1. To this resulting solution were added the surfactant, sodium laureate sulfate (LESS), and Hydrofluoric acid (HF, Sigma) 10%v/v solution. The mixture was foamed by vigorous agitation. HF was used to catalyze the gelation. The abrupt change in rheological behavior is generally used to identify the gel point in a crude way [15, 16]. The gelation time (Tg) was estimated by visual inspection (unaided with optical magnification) and was defined as the time interval starting at the moment the addition of HF catalyzer and the instant where no more fluidity could be observed by tilting the reaction vessel for 30°. The foams were cast just before gelation in plastic containers and sealed. The foam samples were, basically aged at 40 °C for 72 h and dried at 40 °C for 120 h. The molar fractions of reagents used for composite preparation are presented in Table 1.

Characterization of PVA/BG hybrids

Characterization of structure and morphology

Scanning electron microscopy (SEM/EDS) SEM images were taken from composites of PVA/BG with a JSM 6360LV (JEOL/NORAN) microscope coupled to Energy

Table 1 Mole ratio of reagents used for preparation of polyvinyl alcohol/bioglass hybrid composite

Proportion of phases (wt%) PVA/ inorganic phase	Grade of hydrolysis (%)	Mol ratio			
		TEOS	TEP	$CaCl_2$	HF
60/40	80	1.0000	0.1317	0.6094	0.092303
70/30	80				0.215373
80/20	80				0.738423
60/40	98.5				0.138454
70/30	98.5				0.215373
80/20	98.5				0.370455

Dispersive Spectrometer (EDX, semi-quantitative chemical analysis). SEM photomicrographs were used for evaluation hybrid foam morphology, microstructure, and porosity. Prior to examination, samples were coated with a thin gold film by sputtering using low deposition rate, cooling of substrate and maximum distance between target and sample in order to avoid sample damage. Images of secondary electrons (SE) and backscattered electrons (BSE) were obtained using an accelerating voltage of 10–15 kV.

Barrett–Emmett–Teller (B.E.T.) method The BET method was utilized to calculate the specific surface areas. The pore volume and pore-size distributions were derived from the adsorption branches of the isotherms. Before measurements, PVA/BG hybrids were dried at 40 °C for 48 h under N_2 flow. Then, samples were maintained under vacuum for 12 h at 40 °C for proper degassing (Micromeritics). It is important to point out that only mesopore range was evaluated by this method involving N_2 adsorption–desorption isotherms.

Crystallinity and phase characterization by X-ray diffraction

X-ray diffraction characterization (XRD) patterns were obtained from hybrid PVA/BG samples prepared as crushed powders and films produced of polyvinyl alcohol (PHILIPS, PW1710) using CuKα radiation with $\lambda = 1.54056$ Å. XRD analyses were conducted in the 2θ range from 3.03° to 89.91° with steps of 0.06°. Narrow peaks identified within the scan range were confirmed using the Joint Committee on Powder Diffraction Standards files.

Chemical characterization by FTIR spectroscopy

Fourier transform infrared spectroscopy (FTIR) was used to characterize the presence of specific chemical groups in the PVA and PVA/BG hybrid networks, reflecting the effectiveness of the developed procedure for producing different nanostructured materials. FTIR spectra were obtained within the range between 4,000 cm^{-1} and 400 cm^{-1} (Perkin-Elmer, Paragon 1000), using the diffuse reflectance spectroscopy method (DRIFTS-FTIR). Hybrid samples were milled and mixed with dried KBr powder, then placed in a sampling cup and 64 scans were acquired at 2 cm^{-1} resolution with the subtraction of KBr background. The transmittance FTIR spectrum was also obtained for PVA films cast in round glass molds used as a reference.

Characterization of mechanical behavior

The mechanical behavior of the composites was evaluated by compression tests. Specimens were evenly cut from the most homogeneous region of the foam to form blocks measuring $10 \times 10 \times 7$ mm^3. These cubic foam samples were positioned between parallel plates using equipment EMIC DL 3000 with a crosshead velocity of 0.5 mm $min^{-1}$and a 2,000 N load cell. At least five samples ($n = 5$) of each composite system were measured and the results averaged. The modulus (taken at the maximum modulus before the onset of yield point), yield stress (defined as the end of the linear deformation region) and the corresponding strain at yield were also recorded. The elastic modulus was calculated as the slope of the initial linear portion of the stress–strain curve. The yield strength was determined from the cross point of the two tangents on the stress–strain curve around the yield point.

Cytotoxicity and cellular viability activity by MTT assay

Simulated body fluid (SBF) [17] soaking was used as blocking solution of possible remaining cytotoxicity groups from the sol–gel method. The foams were immersed in 75 mL of acellular SBF in polyethylene flasks, with surface area/volume ratio raging from 0.5 cm^{-1} to 1.0 cm^{-1}. The flasks were place inside an incubator at controlled temperature of 37 °C for 72 h. Once removed from the incubation, the samples were rinsed gently in deionised water, and dried at 25 °C for 48 h. Then, all samples subjected to cytotoxicity assay were previously sterilized by exposure to saturated steam of ethylene oxide.

The cell viability was assessed by the reduction of the MTT (3-[4,5-dimetylthiazole-2-yl]-2,5-diphenyltetrazolium bromide) test. VERO cell monolayers were grown in 96-well microtiter plates. Cell proliferation was measured at 2, 4, 6, and 8 days using MTT assay. MTT reagent was added to each sample and incubated at 37 °C for 4 h. This latter procedure was also performed simultaneously for the control cells grown on plastic. Absorbance was read on a

microplate reader (test wavelength: 540 nm). The background absorbance produced by wells containing no cells was subtracted from all samples.

Results and discussion

Synthesis of PVA/BG hybrids

Synthesis and process control of inorganic–organic hybrids produced via sol–gel route is a rather complex system due to the great number of variables that are usually involved, for instance reagents concentration and miscibility (water, TEOS, TEP and $CaCl_2$), pH changes during the reaction in aqueous medium, proportion ratio between alkoxide precursor and water, temperature, and catalyzer, just to name a few. As a consequence, the properties of final composites are very much depending on these variables. Gelation time (Tg) is often used as an reliable indicative of the overall contribution of processing parameter on products obtained through sol–gel route [15, 16]. In Fig. 1, It is showed the influence in the gelation time by varying the relative PVA concentration in the final BG/PVA hybrid produced. It can be clearly observed that an increase of PVA content from 0% to 80% (pure BG and PVA/BG:80/20, respectively) has caused a simultaneous raise on the gelation time from approximately 7 min to over 25 min. Such effect would represent ~400% increase on the time required to have an abrupt change on the viscosity of the reaction medium.

The overall sol–gel process, as the name implies, usually involves two stages: precursors initially form high molecular weight but still soluble poly-intermediates, a sol, and the intermediates further link together to form a 3D network, a gel [15]. Hence, by increasing the PVA concentration in the mixture during the sol–gel reaction, it is reasonable to think that the polymer chain would limit and hinder the interaction among silanol groups of silicates nucleus and polysiloxanes just produced by hydrolysis, causing an increase on the time for the formation of a gel (Tg). Such trend of raising Tg is more pronounced on the PVA with high degree of hydrolysis (PVA-98.5) than on the low degree (PVA-80) due to the formation of hydrogen bonds between hydroxyls of PVA chain and silanol from hydrolyzed alkoxides precursors (TEOS). On the other hand, PVA-80 presents a higher amount of acetate groups, regulating the extension of interaction of PVA hydroxyls with silanol groups and weakening the hydrogen bonding. Thus, in this work, by controlling the concentration ratio of bioactive glass to PVA and also its degree of hydrolysis, it was possible to alter the resulting foam porosity, pore size distribution and interconnectivity.

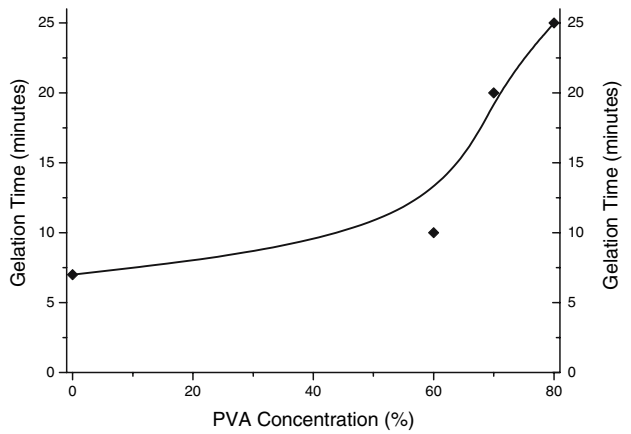

Fig. 1 Effect of polymer concentration on the gelation time for composites prepared with PVA of high degree of hydrolysis (PVA-98.5)

Characterization of PVA/BG hybrids

Characterization of structure and morphology by SEM and B.E.T. method

The pore morphology and distribution of macroporous glass/PVA hybrids can be visualized by the SEM photomicrographs presented in Fig. 2. It can be observed that 3D hybrid scaffolds with interconnected macropores ranging from 10 μm to 600 μm were produced by foaming a mixture of PVA aqueous solution and bioactive glass sol–gel precursors, with the aid of the LESS surfactant.

For each composition the pore network of the hybrid materials can be altered by the synthesis parameters such as concentration of the polymer solution used, concentration of surfactant and casting time. For the same processing conditions and parameters, there was no detectable variation for both modal macropore diameter (~600 μm) and the range of pore size distribution as the content of the glass phase was increased from 20 wt% to 30 wt%, as showed in Fig. 2a, b, respectively. However, a significant increase on the number of pore ranging from 20 μm to 100 μm was found in hybrid with silica content of 40%, as it can be observed in Fig. 2c (arrow) when compared to lower inorganic phase samples (Fig. 2a, b). No major difference was verified on the large pore size with average diameter of approximately 600 μm. Such difference is attributed to the reduction of flexibility of the O–I structure formed by increasing the glass content. Thus, the composite would be consolidated into a more rigid microstructure during the sol–gel reaction process stabilizing smaller bubbles present in the foam mixture. Although the data obtained by SEM micrographs are useful in comparing the macropore structure of the different materials, and how it is affected by processing and composition, it must be said that they are not absolute values but relative results. An important fact

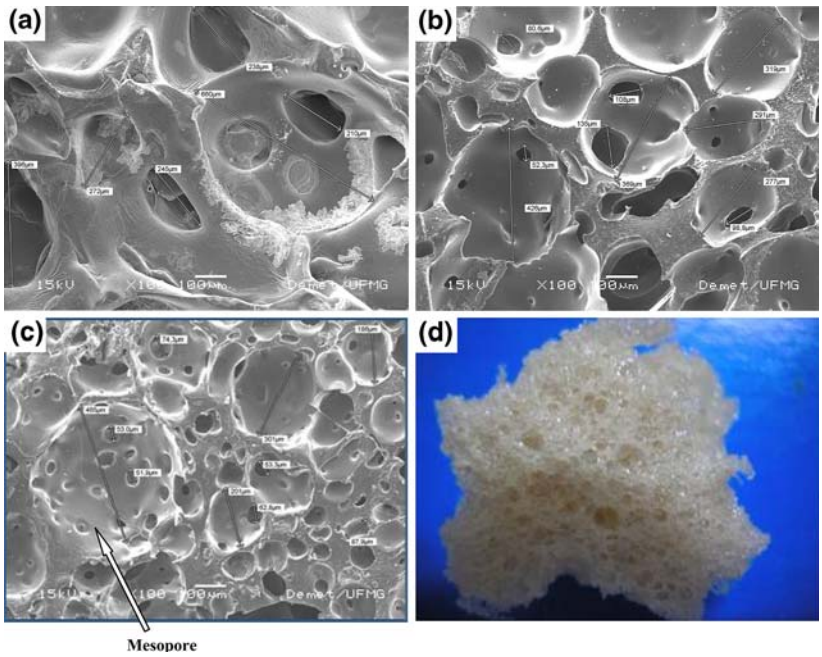

Fig. 2 SEM photomicrographs of hybrids (**a**) 80PVA–20BG, (**b**) 70PVA–30BG, (**c**) 60PVA–40BG and (**d**) optical photograph (no magnification) of 3D scaffold sample

to be mentioned is that a crack-free 3D highly macroporous scaffold was produced by the novel developed PVA/BG stoichiometry proportion via sol–gel route in this work. This is a major achievement compared to some papers reported in the literature [16] where the brittle and fragile behavior of glass derived bioceramic and composites have drastically restricted their application in bone engineering due to the mechanical properties.

In summary, the pore structure obtained is suitable for bone tissue engineering by exhibiting a homogeneous macroporous network with multimodal pore size distribution, namely in the 10–600 μm range, open pores and some interconnectivity. Such hierarchical structure has potential application for future bone tissue ingrowth and nutrient delivery to center of the regenerated tissue [6–8].

By varying the ratio of the organic and inorganic phases, we were able to alter textural and morphological properties and porosity. The foams exhibited high porosity in the range from 65% to 80% (Fig. 2d), estimated by using Eq. 1, where the apparent density (ρ) of the scaffolds was determined by using the measured mass and volumes of the scaffolds and (ρ_0) is the density of the non-porous material.

$$P = 1 - \frac{\rho}{\rho_0} \tag{1}$$

The specific surface area of hybrid scaffolds was estimated by the BET method from the nitrogen adsorption–desorption isotherms. For the hybrids samples with compositions of 70%PVA–30%BG the results showed that as the PVA hydrolysis grade was increased from 80% to 98.5%, the average surfaces area of the scaffolds decreased almost 50%, from 3.0 $m^2\ g^{-1}$ to 1.6 $m^2\ g^{-1}$ (Fig. 3). It must be said that BET method is not suitable for macroporous evaluation. In fact, it was used only as reference values and as complementary technique for morphology analysis (SEM). In a previous paper of our group [18] porosity has been addressed through other methods, based on high bioactive glass content in the hybrid formation.

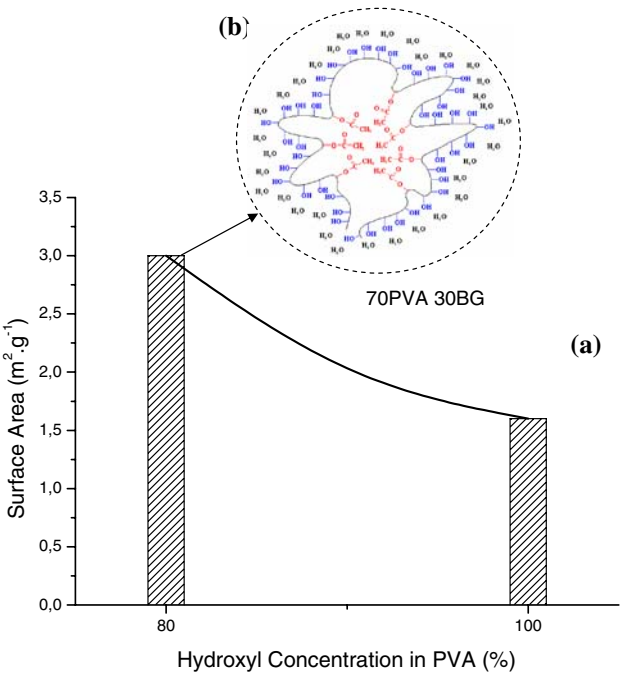

Fig. 3 Effect of degree of hydrolysis of PVA on the resulting surface area estimated by BET for hybrid PVA/BG:70/30

It can be attributed to the development of a higher number of hydrogen bonds between hydroxyl groups of PVA chain (PVA-98.5) with the remaining silanol present on the glass surface, causing the formation of a uniform polymer film "capping" the silicates domains. Thus, that would reduce the occurrence of mesopores in the nanometer scale (2–50 nm). On the other hand, by keeping constant the PVA/BG ratio and reducing the degree of hydrolysis in PVA chain has the opposite effect, representing an increase on the relative number of acetate groups raising the overall surface area (Fig. 3b) due to the formation of mesopores. In Fig. 3b is showed the schematic representation of the balance of charge of a partially hydrolyzed PVA would be stabilized by adopting a conformation, where acetate groups are oriented to the center and hydroxyls to the outer part of the molecule in a hydrophilic medium [19–22].

Chemical characterization by FTIR spectroscopy

The main vibrational bands associated with both PVA and bioactive glasses ($SiO_2CaOP_2O_5$) are presented in Table 2. Representative IR spectra of the pure PVA films, the bioactive glass and the hybrid foams (PVA/BG: 70/30%) are showed in Fig. 4, for the sample group of PVA almost fully hydrolyzed (PVA-98.5), and in Fig. 5 for the PVA-80 hydrolyzed sample group. Although not showed in the figures, the spectra of the other hybrids obtained in this work are very similar to the spectra exhibited in Figs. 4c and 5c. In Figs. 4a and 5a, FTIR spectra of pure PVA are showed. As it can clearly observed in Figs. 4 and 5, the degree of hydrolysis of both PVA used on the process have indicated different FTIR spectra.

For both PVA spectra, the broad band observed from 3,100 cm^{-1} to 3,600 cm^{-1} may be assigned to O–H stretching due the strong hydrogen bond of intramolecular and intermolecular type [19–22]. The presence of a higher hydroxyl content in the almost fully hydrolyzed PVA compared to the PVA 80% hydrolyzed can be seen from the broader band around 3,300 cm^{-1}. The C–H alkyl stretching band can be observed at 2,850–2,950 cm^{-1}. The absorption peaks at approximately 1,710 cm^{-1} (for highly hydrolyzed PVA) or 1,740 cm^{-1} (for 80% hydrolyzed) and at 1,090–1,150 cm^{-1} may be attributed to the stretching vibration of νC=O and C–O of the remaining vinyl acetate non-hydrolyzed group of PVA polymer [19–22]. The absorption band around 1,700 cm^{-1} arises due to the carbonyl band (C=O) of the acetate group found in partially hydrolyzed PVA polymer and has higher relative intensity for the PVA 80% hydrolyzed as expected from the higher concentration of remaining acetate groups. The relative crystallinity of two PVA samples with different degree of hydrolysis was verified by the presence of the vibrational band at ν = 1,141 cm^{-1}. It was clearly noted that PVA with high degree of hydrolysis (PVA-98.5, Fig. 4a) has showed a stronger intensity on this band when compared to low degree of hydrolysis (PVA-80, Fig. 5a). That means, as the number hydroxyl groups are increased the number of stabilizing hydrogen bonds are simultaneously raised, resulting in a more crystalline polymer network structure [20–22].

In the FTIR spectrum of the bioactive glass presented in both figures (Figs. 4b, 5b), the vibrational modes due to Si–O–Si asymmetric stretching are observed at approximately 1,070 and 1,200 cm^{-1}. Additional peaks are seen at 790 cm^{-1} (for symmetric Si–O–Si stretching vibration, and

Table 2 Major FTIR vibrational bands associated with PVA and bioactive glass

Material	Wave number (cm^{-1})	Position assignment	References
BG	461	Si–O–Si stretching	[23]
BG	822	Symmetric Si–O–Si stretching	[21]
PVA	850	C–C stretching	[22]
PVA	916	(CH)–CH_2 bending	[22]
BG	953	Si–OH bond stretching	[19, 22]
BG	1,000–1,220, 960 doublet at ν = 569 and ν = 603	Phosphates (PO_2^-, PO_3^{-2}), (PO_4^{-3})	[24]
BG	1,080	Asymmetric Si–O–Si stretching in SiO_4 tetrahedron	[19, 23]
PVA	1,093	(C–O)–C–OH bending	[20]
PVA	1,141	C–O stretching, crystallinity	[20]
PVA	1,329	(OH)–C–OH bending	[20]
PVA	1,461–1,471	(CH)–CH_2 bending	[20]
BG, PVA	1,634	O–H bending (molecular water)	[20, 22]
PVA	2,937–2,870	CH stretching	[20]
PVA	1,710–1,740	C=O stretching, acetate groups	[19–22]
BG, PVA	3,550–3,200	O–H stretching and adsorbed water	[20, 22]

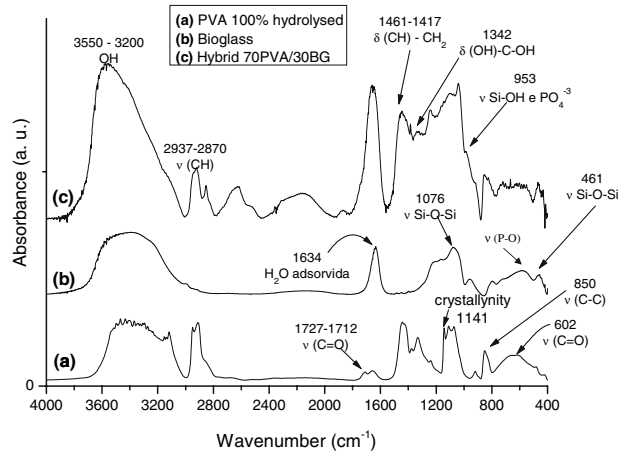

Fig. 4 FTIR spectra of sample: (**a**) polyvinyl alcohol, PVA-98.5% hydrolyzed, (**b**) bioactive glass and (**c**) hybrid 70 wt%PVA–30 wt%BG

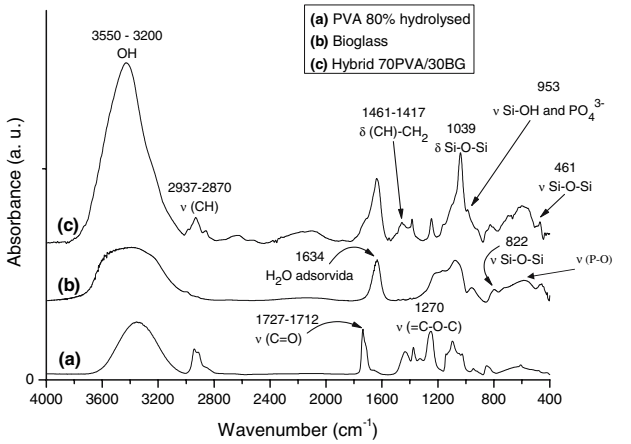

Fig. 5 FTIR spectra of sample: (**a**) polyvinyl alcohol, PVA-80% hydrolyzed, (**b**) bioactive glass and (**c**) hybrid 70 wt%PVA–30 wt%BG

at 450 cm^{-1} (for Si–O–Si bending modes) [21–23]. A typical absorption band observed in silica gel is located at 1,640 cm^{-1} and is attributed to the deformation mode of adsorbed molecular water in the pores. The band at 950 cm^{-1} has been ascribed to the stretching vibration of silanol groups in pure silica (vibrational modes of Si–O-stretching) [23].

FTIR spectra of composite with composition of 70 wt%PVA–30 wt% bioactive glass (PVA/BG) are presented in Figs. 4c and 5c, for PVA with 98.5% and 80% hydrolyzed, respectively. The bioglass component is identified by major vibration bands, (Si–O–Si, at 1,080 and 450 cm^{-1}). For both hybrids, the peak at 950 cm^{-1} associated with the Si–OH vibrational mode remains as a shoulder. In the frequency range of 3,000–3,650 cm^{-1}, a broader band was noted, especially for hybrid prepared from PVA almost fully hydrolyzed (Fig. 4c). The band located at 1,640 cm^{-1} remains in the spectra of the hybrids since the low heating temperature is not enough to remove the molecular water of the pores. The terminal vinyl groups of the PVA which appear at 1,710 cm^{-1} (for almost fully hydrolyzed PVA) or 1,740 cm^{-1} (for 80% hydrolyzed) are not showed in the hybrids, which suggests that these bonds might be involved in crosslinking with silica. In the range 1,500–900 cm^{-1} there is a superposition of the bands derived from the bioglass and the PVA components [20–22]. The band at 476 cm^{-1} is assigned at the Si–O–Si bending mode and the shoulder at 950 cm^{-1} is related to the Si–OCa vibration mode. Also, typical phosphate group bands at ν = 1,000–1,220 cm^{-1} (PO_2^-, PO_3^{-2}) and ν = 960 cm^{-1} (PO_4^{-3}). The FTIR spectra of samples containing P showed in addition a doublet at ν = 569 and ν = 603 cm^{-1}, which is associated with the stretching vibrations of phosphate groups related to the presence of crystalline phosphates in the glasses [24]. In summary, FTIR spectroscopy has proven to a very powerful tool on investigating the formation of PVA/BG hybrids and to how organic–inorganic network is structured.

Crystallinity and phase characterization by X-ray diffraction

The X-ray diffraction analysis result for the pure bioactive glass is showed in Fig. 6a. As expected, it did not show the presence of any crystalline phases, being a totally amorphous phase. On the other hand, the XRD patterns from both pure PVA samples, low degree (PVA-80) and high

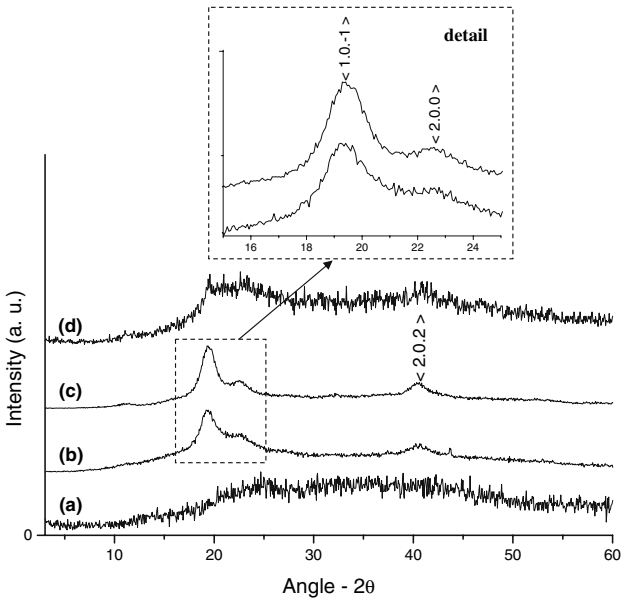

Fig. 6 XRD patterns of (**a**) bioactive glass $SiO_2CaOP_2O_5$, (**b**) PVA 80% hydrolyzed, (**c**) PVA 98.5% hydrolyzed and (**d**) hybrid 70 wt%PVA–98.5 hydrolyzed–30 wt%BG

degree of hydrolysis (PVA-98.5), are presented in Fig. 6b, c, respectively. They have both being identified as a semi-crystalline structure, with slightly higher crystallinity for the PVA-98.5 due to the superior concentration of hydroxyls groups (Fig. 6c, insert). This XRD results have endorsed the previous findings based on FTIR spectrum of PVA with high degree of hydrolysis (section "Chemical characterization by FTIR spectroscopy"). The XRD curve for PVA–BG hybrid (PVA/BG:70/30) synthesized is showed in Fig. 6d. It can be easily verified the sum up of both contributions from PVA with semi-crystalline structure and amorphous phase of bioactive glass. That would be a typical composite XRD pattern showing contribution from all components.

Characterization of mechanical behavior

An initial assessment of the mechanical behavior of the hybrid materials produced was done at room temperature by axially compression test with samples prepared using the two PVA hydrolysis grade in the composition 70 wt% PVA–30 wt% bioactive glass (PVA/BG:70/30). The compression tests results of PVA/BG hybrids are presented in Fig. 7, where PVA-80 is presented in Fig. 7a and PVA-98.5 in Fig. 7b. Both curves have showed a similar behavior pattern, with the compressive stress consisted of an initial Hookean region in which stress increased in proportion to strain due to compression of the cell elements followed by a plateau region representing plastic collapse and densification, corresponding to collapse of the cells throughout the material with subsequent loading of the cell edges and faces against one another, as described by Gibson and co-workers [25]. The averaged elastic modulus of hybrids ranged roughly from 2.6 MPa to 6.0 MPa, PVA-80 and PVA-98.5, respectively. The summary of mechanical

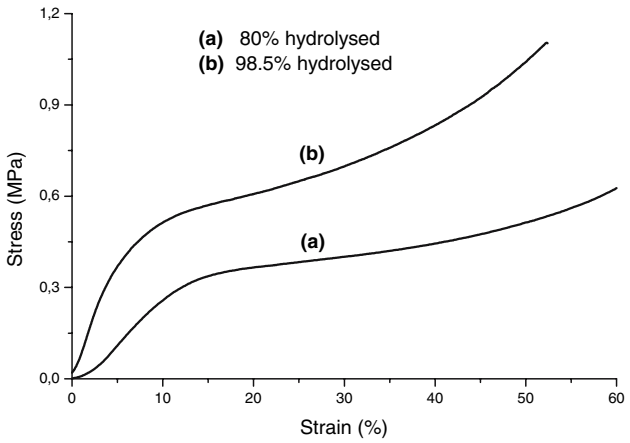

Fig. 7 Stress–strain curves obtained by compression test of hybrids of 70PVA30BG prepared with polymer (**a**) 80% hydrolysis grade and (**b**) 98.5% hydrolysis grade

Table 3 Data for the axial compression modulus, yield stress and strain at yield for the hybrids PVA–bioactive glass, obtained with PVA-98.5 and partially hydrolyzed (PVA-80)

Proportion of the phases (wt.%) PVA/inorganic	Grade of hydrolysis (%)	Axial yield stress (MPa)	Axial yield strain (%)	Axial modulus (MPa)
70/30	80.0	0.27 ± 0.02	10.9 ± 3.5	2.6 ± 0.6
	98.5	0.29 ± 0.03	5.0 ± 0.9	5.9 ± 1.4
Cancellous bone [25, 26]		–	–	2–12

tests performed and reference values found in the literature for cancellous bone are showed in Table 3.

The handling strength of pure glass samples (BG) produced was too low, very fragile and brittle, and therefore not considered suitable for comparison [18]. Hence, the PVA polymer introduced into hybrid composite has tremendously increased the mechanical properties over the pure macroporous bioactive glass produced by sol–gel method. It should be emphasized that the PVA-98.5 with high degree of hydrolysis has presented a much superior values of all mechanical properties (Fig. 7b) when compared to PVA-80 (Fig. 7a), with maintaining the PVA/BG ratio constant. That leads to a very important conclusion, that in fact, the interface PVA–BG has a stronger interaction of hydroxyls from PVA and silanol from BG as the degree of hydrolysis is increased. In addition, it is reported in the literature that the higher the degree of hydrolysis of PVA and the polymer M_w the higher is the mechanical properties [19, 20].

Based strictly on these mechanical properties reported, one may assume that the PVA/BG developed in the present work are suitable for partial replacement of damaged cancellous bone tissue which has typically a broad range of modulus from 2 MPa to 12 MPa [26, 27].

Cytotoxicity and cellular viability activity by MTT assay

The cell viability, assessed by the MTT assay, is presented in Fig. 8. The cells treated with extracts of hybrid foams as prepared showed relatively good cell viability compared to the control. The cell viability of all experimental groups was not significantly altered either by the PVA/BG ratio cells or the degree of hydrolysis of PVA used in the composite.

The preparation method of PVA/BG composite prior to be submitted to MTT test has successfully reduced or even eliminated the expected high toxicity level of the sol–gel derived hybrid materials that not subjected to stabilizing and cleaning procedures [18].

We should point out that further investigation is under way where direct contact of cell culture spreading onto

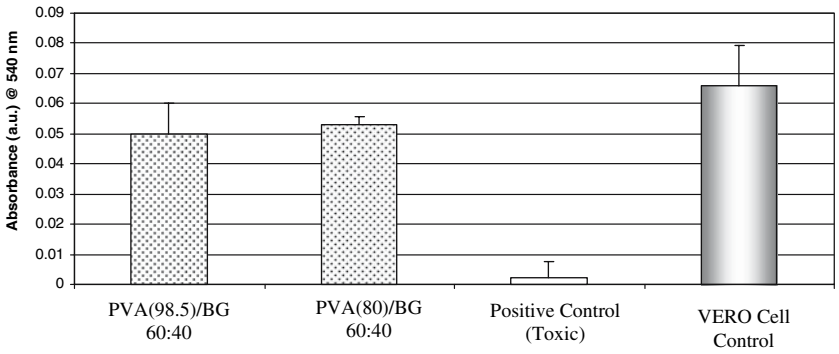

Fig. 8 Relative cell viability of VERO cells cultured with extracts of PVA, BG and hybrid PVA/BG samples as prepared. Simultaneous cultures were incubated with complete culture medium only as negative control (NC)

PVA/BG hybrids for a more solid results regarding to mimic the in vivo environment of bone tissue replacement.

Conclusions

A 3D macropore structure composed of PVA/BG was successfully synthesized by the sol–gel route with the aid of the LESS surfactant. These hybrid foams exhibit a hierarchical structure with interconnected macropores (10–500 μm) and a mesoporous framework typical of gel-glasses (pores of 2–50 nm). The resultant hybrids exhibit excellent mechanical strength that was significantly influenced by the hydrolysis grade of PVA utilized, where an increase in the hydrolysis grade has improved the mechanical properties of the composite. The mechanical properties of some of the obtained composites had values comparable with the ones reported for cancellous bone. Also, the cell viability of all experimental groups was not significantly altered either by the BG/PVA ratio cells or the degree of hydrolysis of PVA used in the composite. Hence, this new class of composite material combines large pores to support vascularization and 3D tissue growth with the ability that bioactive materials have to provide bone-bonding and controlled release of ionic biologic stimuli to promote cell proliferation of bone tissue.

Acknowledgements The authors acknowledge National Council for Scientific and Technological Development (CNPq) and State of Minas Gerais Research Foundation (FAPEMIG) for financial support on this project. We are also grateful to Prof. Dr. Dagoberto Santos for the facilities of Electronic Microscopy Laboratory and Dr. Vilma Costa for the kind assistance on sol–gel processing.

References

1. Kim HM (2003) Curr Opin Solid State Mat Sci 7:289
2. Nissan BB (2003) Curr Opin Solid State Mat Sci 7:283
3. Tadic D, Beckmann F, Schwarz K, Epple M (2004) Biomaterials 25:3335
4. Jones JR, Hench LL (2003) Curr Opin Solid State Mat Sci 7:301
5. Olivier V, Faucheux N, Hardouin P (2004) Drug Discov Today 9:803
6. Burg KJL, Porter S, Kellam JF (2000) Biomaterials 21:2347
7. Rezwan K, Chen QZ, Blaker JJ, Boccaccini AB (2006) Biomaterials 27:3413
8. Hench LL (1991) J Am Ceram Soc 74:1487
9. Jones RJ, Ehrenfried LM, Hench LL (2005) Biomaterials 27:964
10. Pereira MM, Jones JR, Orefice RL, Hench LL (2005) J Mater Sci: Mater Med 16:1045
11. Chiellini E, Corti A, D'antone S, Solaro R (2003) Prog Polym Sci 28:963
12. Pereira APV, Wander LV, Orefice RL (2000) J Non-Cryst Solids 273:180
13. Paul W, Sharma CP (2006) Am J Biochem Biotechnol 2(2):41
14. Yamaoka T, Tabata Y, Ikada Y (1995) J Pharmaceut Pharmacol 47:479
15. Brinker CJ, Scherer GW (1990) Sol–gel science: the physics and chemistry of sol–gel processing. Academic Press, New York, NY
16. Oki A, Qiu X, Alawode O, Foley B (2006) Mater Lett 60:2751
17. Kokubo T (1998) Acta Mater 46:2519
18. Pereira MM, Jones JR, Hench LL (2005) Adv Appl Ceram 104(1):35
19. Mansur HS, Oréfice RL, Mansur AAP (2004) Polymer 45:7193
20. Andrade G, Barbosa-Stancioli1 EF, Piscitelli Mansur AA, Vasconcelos WL, Mansur HS (2006) Biomed Mater 1:221
21. Mansur HS, Oréfice RL, Vasconcelos WL, Lobato ZP, Machado LJ (2005) J Mater Sci: Mater Med 16:333
22. Coates J (2000) In: Meyers (ed) Encyclopedia of analytical chemistry. Wiley, Chichester, pp 10815–10837
23. Almeida RM, Pantano CG (1990) J Appl Phys 68:1225
24. Roman J, Padilla S, Vallet-Regı M (2003) Sol–gel glasses as precursors of bioactive glass ceramics. Chem Mater 15:798; Pereira MM, Clark AE, Hench LL (1994) J Biomed Mater Res 28:693
25. Gibson LJ (2005) J Biomech 38:377
26. Shi D, Jiang G (1998) Mater Sci Eng C 6:175–182
27. Montjovent MO, Mathieu L, Hinz B, Applegate LL, Bourban PE, Zambelli PY, Manson JA, Pioletti DP (2005) Tissue Eng 11:1640